Anomalous $N_{4,5}P_1P_1$ Auger decay from the $4d$ photoionization states in atomic barium

J. Nikkinen,[1] H. Aksela,[1] S. Heinäsmäki,[1] S. Fritzsche,[1,2] E. Kukk,[1] M. Huttula,[1] and S. Aksela[1]
[1]*Department of Physical Sciences, University of Oulu, P.O. Box 3000, 90014 University of Oulu, Finland*
[2]*Department of Physics, University of Kassel, Heinrich-Plett-Strasse 40, D-34132 Kassel, Germany*
(Received 10 May 2002; published 27 December 2002)

The $4d$ photoionization and subsequent $N_{4,5}P_1P_1$ Auger decay in free barium atoms have been investigated with special emphasis on the anomalous intensity ratio in the Auger electron spectrum. In order to understand the details of the spectrum, a series of *ab initio* calculations based on the multiconfiguration Dirac-Fock method have been performed. Theoretical predictions are compared with high-resolution electron spectra measured using synchrotron radiation. An interference effect, induced through electron correlation, was found to give rise to the anomaly of the intensities.

DOI: 10.1103/PhysRevA.66.064703 PACS number(s): 32.80.Hd, 32.80.Fb

Photoionization from the $4d$ subshell has proven to be fruitful in studying many-electron phenomena in free Ba atoms [1–5]. In the simple shell model the $4d$ photoelectron spectrum (PES) should consist of just two peaks due to the spin-orbit splitting of the $4d_{5/2}$ and $4d_{3/2}$ holes, with an intensity ratio of about 3:2. For Ba, however, the single-particle central field model breaks down as a consequence of the collapse of the outer orbitals during the $4d$ ionization. This collapse, which is particularly important for the $4f$ and $5d$ orbitals, is induced by a strong increase of the effective charge experienced by the outer electrons in the ionization process.

The $N_{4,5}P_1P_1$ Auger electron spectrum (AES) is also known to display interesting phenomena [3]: The final ionic state of the Auger decay ($[\mathrm{Kr}]4d^{10}5s^25p^6, J_f=0$) is an almost pure state in jj coupling. So the AES could be assumed to be a mirror image of the $4d$ PES, weighted by the corresponding Auger intensities. Nevertheless, the intensity ratio in the AES differs dramatically from the corresponding intensity ratio of 3:2 in the PES [3]. This anomaly is a clear sign of strong electron correlation.

To clarify the origin of this anomaly in the AES, we made as a first step a series of multiconfiguration Dirac-Fock (MCDF) calculations to explore the dependence of the $4d$ partial photoionization cross sections on the size of the wave function expansions. In the second step, Auger component rate calculations from different $4d^{-1}$ intermediate ionic states were carried out. Finally, high-resolution synchrotron radiation measurements were performed for both the photoionization and the Auger decay, and a comparison of the experimental results with theoretical simulations is presented in this report. The details of the calculations in best agreement with experiment are given in order to classify the main factors behind the observed behavior of the intensities.

The measurements of the $4d$ PES and the subsequent $N_{4,5}P_1P_1$ AES of Ba vapor were carried out at the high-resolution gas phase undulator beamline I411 at the 1.5 GeV MAX II storage ring in Lund, Sweden. Radiation was monochromatized by an SX-700 plane grating monochromator to 138.0 eV photon energy, which was calibrated using the Xe $4d$ photolines [6]. Ejected electrons were recorded with a rotatable SES-100 hemispherical electron analyzer at a constant pass energy of 20 eV at an emission angle of 54.7° with respect to the electric-field vector, in the plane perpendicular to the propagation direction of the linearly polarized photon beam. The kinetic energy scale of the analyzer was determined from the Xe $N_{4,5}OO$ Auger lines [6] and the energy resolution, approximately 60 meV, from the Xe $5p$ photolines. A resistively heated stainless steel vapor oven was used to produce an intense atomic beam of Ba in the collision area.

The experimental $4d$ PES and $N_{4,5}P_1P_1$ AES are plotted in Fig. 1. The intensities of the spectra have been normalized by setting the peaks numbered 6 equal. Both spectra were fitted using Voigt profiles with fixed instrumental broadening represented by a Gaussian width of 68 meV in the PES and 60 meV in the AES. The Lorenzian linewidths of 100 $\pm$20 meV were obtained from the fit for the main peaks 1, 2, and 6. The satellite structure of the PES is almost completely due to configuration interaction, where the peaks 1–4 can be assigned as originating from $4d_{5/2}$ ionization and peaks 5–9 from $4d_{3/2}$ ionization [5]. The intensity ratio (R_P) between the $4d_{5/2}$ and $4d_{3/2}$ photoelectron peaks was found to be approximately 1.2 and the corresponding ratio (R_A) in the AES 0.7. In this work we will mainly focus on the three main peaks, labeled as 1, 2, and 6. In the AES peak 1 vanishes almost completely but the relative intensity of peak 2 is only slightly reduced with respect to the peak 6. In previous studies the detection of this kind of detail was prevented by moderate resolution.

In this section we briefly summarize the theory given in [3]. The $N_{4,5}P_1P_1$ Auger transition in Ba, induced by ionization of randomly oriented atoms by linearly polarized light, is

$$[\mathrm{Kr}]4d^{10}5s^25p^66s^2+h\nu\rightarrow[\mathrm{Kr}]4d^{-1}5s^25p^66s^2+e^- \rightarrow[\mathrm{Kr}]4d^{10}5s^25p^6+e_A^- \qquad (1)$$

where the number of emitted Auger electrons e_A^- at the magic angle of 54.7° is proportional to the product of the total photoionization cross section and the Auger component rate. By constructing both the ground state and the intermediate ionic state configuration state functions (CSFs) using the same set of orthogonal orbitals we can express the total

relative photoionization cross section, integrated over all directions of the photoelectron, as

$$Q_\beta(J_\beta)=\frac{1}{3}Q'_\beta(J_\beta)\sum_{l,j}\int|\langle n_\alpha l_\alpha j_\alpha\|r^{(1)}\|\epsilon l j\rangle|^2 d\epsilon, \quad (2)$$

where we have used the dipole approximation and assumed that the ionization takes place from an inner filled subshell. In Eq. (2) the continuum orbitals have been evaluated in an average jj potential of the intermediate ionic state configurations by keeping the bound orbitals fixed. The first term in Eq. (2) is the partial relative photoionization cross section

$$Q'_\beta(J_\beta)=(2j_\alpha+1)\left|\sum_\nu\sum_\alpha c_{\beta\nu}c_{i\alpha}\delta_{X\nu Y\alpha}\right|^2 \quad (3)$$

with X_ν referring to the configuration associated with $\Phi_\nu(J_\beta)$ and Y_α referring to the same parent configuration after coupling an $n_\alpha j_\alpha$ orbital from $\Phi_\alpha(J_i)$. The Auger component rate is

$$T_{f\beta}(J_f,J_\beta)=\frac{2\pi}{\hbar}\sum_{l_A,j_A}\left|\sum_\mu\sum_\nu c_{f\mu}c_{\beta\nu}M^{\mu\nu}_{f\beta}\right|^2 \quad (4)$$

where $M^{\mu\nu}_{f\beta}=\langle\Phi_\mu(J_f)\epsilon_A l_A j_A;J_\beta\|V\|\Phi_\nu(J_\beta)\rangle$. In Eq. (4) the final ionic state CSFs $\Phi_\mu(J_f)$ have been coupled to the energy normalized continuum orbitals $|\epsilon_A l_A j_A\rangle$ of the Auger electron to yield antisymmetrized wave functions with the same parity as the intermediate ionic state CSFs $\Phi_\nu(J_\beta)$. In addition, by assuming that the total decay rate $P_\beta(J_\beta)$ of the intermediate ionic states is independent of β and J_β, the relative number of emitted Auger electrons is

$$n_{f\beta}(J_fJ_\beta)=T_{f\beta}(J_f,J_\beta)Q'_\beta(J_\beta). \quad (5)$$

In this paper all the bound state wave functions were generated by the MCDF method using the GRASP92 package in the average level (AL) scheme [7]. The Auger component rates and continuum wave functions are determined using the RATIP package [8]. Because in this work we are interested in the formation of the main $4d^{-1}$ intermediate ionic states and their decay channels, it is useful to neglect both the ground state and final ionic state configuration interaction (CI) due to their weak effect on the corresponding intensities. The ground state of Ba was found to be dominated to over 90% by the CSF $([\mathrm{Kr}]4d^{10}5s^25p^66s^2,J_i=0)$ and correspondingly the final ionic state of the $N_{4,5}P_1P_1$ Auger transition to over 90% by the CSF $([\mathrm{Kr}]4d^{10}5s^25p^6,J_f=0)$.

Intermediate ionic state atomic state functions (ASFs) were generated using the following two basis sets: (A) $4d^{-1}(4f,5d,6s,6p)^2$ and (B) $4d^{-1}(4f,5d,6s,6p,6d,7s,7p)^2$. Below we report results of three types of calculations. The results obtained with the basis set (A) are referred as PES-A and AES-A, and the results with set (B) as PES-B1 and AES-B1. In a separate calculation with the basis set (B), the radial wave functions were taken from the calculation (A) and the radial wave functions other than $(4f,5d,6p,6d,7s,7p)$ were frozen. The results obtained this way are referred as PES-B2 and AES-B2. The basis set (A) was chosen as a starting point following the earlier work [3]. To allow a more accurate description of the Auger part of the spectrum, the basis set was expanded to (B). Convergence problems associated with large MCDF calculations led to the conclusion that no significant advantage can be obtained from further extensions. In AL calculations, such as (B1), which involve large numbers of CSFs, the orbitals obtained are good only for the states located close to the average energy. Taking in (B2) the orbitals for the ''passive'' electrons from a smaller calculation (A), which, however, predicts the important features of the photolelectron spectrum rather well, allows a more accurate computation of the important outer-shell electrons participating in the Auger decay process.

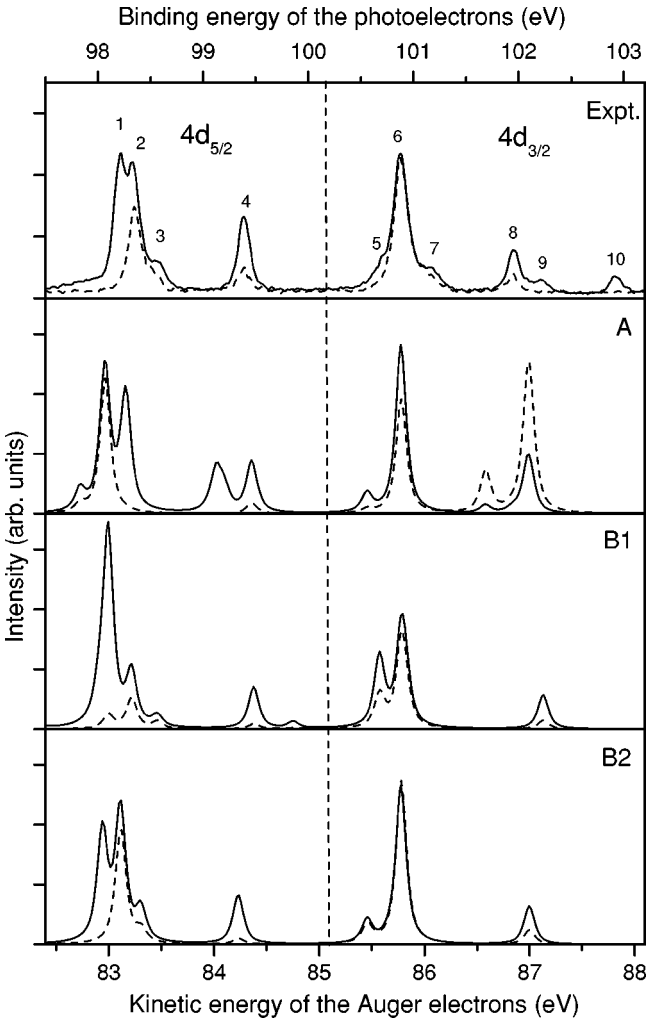

FIG. 1. Experimental (Expt.) and calculated (A, B1, B2) $4d$ PES (solid line) and $N_{4,5}P_1P_1$ AES (dashed line) for Ba. The relative intensities of the calculated PES and the AES have been fixed by setting the peaks number 6 equal in (B2) and using the same scaling in calculations (A) and (B1). All calculated spectra have been generated with experimental line widths and the energies are fixed to the experimental spectrum using the peak number 6.

The calculated PES-A (solid line) and the corresponding AES-A (dashed line) are shown in Fig. 1(A). Even though the main features of the PES-A spectrum are close to the experimental spectrum, the AES-A deviates drastically from

TABLE I. Main factors in the Auger rates of peaks 1, 2, and 6.

Label	$\Phi_\nu(J_\beta)$	$M_{f\beta}^{\mu\nu}$	Peak 1		Peak 2		Peak 6	
			$c_{\beta\nu}$	$c_{f\mu}c_{\beta\nu}M_{f\beta}^{\mu\nu}$	$c_{\beta\nu}$	$c_{f\mu}c_{\beta\nu}M_{f\beta}^{\mu\nu}$	$c_{\beta\nu}$	$c_{f\mu}c_{\beta\nu}M_{f\beta}^{\mu\nu}$
a	$4d_{5/2}^{-1}6s^2, J_\beta=5/2$	0.0007	0.55	0.0004	0.60	0.0004		
b	$4d_{5/2}^{-1}(5d_{5/2}^2, J=0)J_\beta=5/2$	-0.0045	-0.39	0.0017	-0.12	0.0005		
c	$4d_{5/2}^{-1}(5d_{5/2}^2, J=4), J_\beta=5/2$	-0.0112	0.21	-0.0023	-0.40	0.0043		
d	$4d_{5/2}^{-1}(5d_{5/2}^2, J=2), J_\beta=5/2$	-0.0090	0.08	-0.0007	-0.21	0.0018		
e	$(4d_{3/2}^{-1}5d_{3/2}^1, J=0)5d_{5/2}^1, J_\beta=5/2$	0.0135	0.04	0.0005	-0.22	-0.0029		
f	$4d_{3/2}^{-1}6s^2, J_\beta=3/2$	0.0007					0.80	0.0006
g	$4d_{3/2}^{-1}(5d_{3/2}^2, J=0), J_\beta=3/2$	-0.0055					-0.22	0.0012
h	$4d_{3/2}^{-1}(5d_{3/2}^2, J=2), J_\beta=3/2$	-0.0103					-0.13	0.0013
	Sum of all positive $c_{f\mu}c_{\beta\nu}M_{f\beta}^{\mu\nu}$			0.0040		0.0083		0.0060
	Sum of all negative $c_{f\mu}c_{\beta\nu}M_{f\beta}^{\mu\nu}$			-0.0041		-0.0046		-0.0017

the experimental one. However, the smearing out of the doublet structure of the $4d_{5/2}$ peaks 1 and 2 in passing to the AES is reproduced. The calculated PES-B1 and AES-B1 are presented in Fig. 1(B1). The PES-B1 and AES-B1 results are in worse correspondence with the experiment than the PES-A and AES-A results, which can be understood to result from deviation of the average energy from the energies of the important levels. The PES-B2 and the AES-B2 results, presented in Fig. 1(B2), give quite a good description of both the photoionization and the Auger decay, as is seen by comparing the results to the experimental spectra. The doublet structure in the PES, and even peak 3, are very well reproduced, as well as the change in this structure in passing to the AES. Note that the structures 1–3 in the AES are much better predicted by AES-B2 than by AES-A, even though the corresponding calculated PESs are rather similar. This indicates higher sensitivity of the AES to the quality of the orbital wave functions and electron correlation.

The ratio $R=R_P/R_A$ which reduces to a photon energy independent ratio of the Auger component rates [Eq. (4)] for the $4d_{3/2}$ and $4d_{5/2}$ structures can be used as a quantitative indicator of the agreement between the calculation and experiment. R was found to be 3.2, 3.7, and 1.6 in calculations (A), (B1), and (B2), respectively, and 1.7 in experiment. Thus the calculation (B2), where the intermediate ionic state CI is properly accounted for, predicts the anomalous intensity ratio in the Auger decay in accordance with experiment. The next step was to clarify where the effect originates from; the overlap of the orbitals, the expansion of the intermediate ionic states, and the sign of the mixing coefficients all play a significant role in the Auger rate calculations. The largest Auger amplitudes as well as those related to CSFs $(4d^{-1}6s^2, J_\beta=3/2,5/2)$ are listed in Table I for the main peaks 1, 2, and 6. The table shows the CSFs, their matrix elements $M_{f\beta}^{\mu\nu}$, mixing coefficients $c_{\beta\nu}$, and Auger amplitudes $c_{f\mu}c_{\beta\nu}M_{f\beta}^{\mu\nu}$. (Note that $c_{f\nu}\simeq 1$.) The sums of all positive and negative Auger amplitudes are also included.

According to the calculations, the largest amplitudes in Auger rates arise from the strong mixing of CSFs of the types $(4d^{-1}5d^2, J_\beta=3/2,5/2)$ in the intermediate ionic states. These CSFs have large weights in the ASF expansion and the Slater integrals $R^k(4d\epsilon d,5d5d)$ are large due to the partial collapse of the $5d$ orbital. The effect due to the collapse of the $4f$ orbital is less significant. Although it gives rise to large Slater integrals of the types $R^k(4d\epsilon d,4f4f)$ and $R^k(4d\epsilon d,4f6p)$, the small weights of the corresponding CSFs result in a small effect on the total Auger rate. The amplitudes originating from CSFs (a) and (f) are also negligible. These CSFs have large mixing coefficients but due to relatively small Slater integrals $R^k(4d\epsilon d,6s6s)$ the amplitude is quite small. Note also that the $4d_{5/2}$ and $4d_{3/2}$ hole configurations are mixed. The CSF (e) with a $4d_{3/2}^{-1}$ character contributes to Auger peaks 1 and 2 which are mainly of $4d_{5/2}^{-1}$ character. The left side of the AES in Fig. 1 can no longer be considered as a clear $4d_{5/2}$ spectrum.

Anomalies in the AES result from destructive and constructive interference effects as follows. For the peak 1 there are two large Auger amplitudes, originating from CSFs (b) and (c). These amplitudes have opposite signs, leading to an almost zero Auger component rate. In addition, the remaining smaller positive and negative terms appear also to cancel each other. For the peak 2 there are three large amplitudes, two positive ones originating from CSFs (c) and (d) and one negative originating from CSF (e). In this case, the total sum of negative amplitudes is insufficient to cancel the positive terms. For peak 6 the most significant amplitudes originate from CSFs (g) and (h), but there is also a large contribution from other positive amplitudes. The total contribution of the negative terms is rather small compared to the positive one.

In conclusion, a high-resolution experimental study combined with MCDF calculations have allowed us to understand the processes leading to an intensity reversal in passing from the PES to the AES. The effect occurs as a consequence of strong electron correlation. When the orbitals experiencing the collapse are involved in Auger decay through CI, large Auger amplitudes with positive and negative signs are created. These strengthen or weaken the Auger rate as a CI-induced interference takes place. The effect will occur in situations with strong intermediate ionic state CI, and may also affect the total Auger rates. Systematic studies of the PES and the AES and of the total decay widths of other atoms similar to Ba will allow one to see whether the mecha-

nism responsible for the anomalous Auger decay ratio persists in other systems also. As seen here, the PES alone is not enough to study CI in intermediate ionic states; the AES is of crucial importance. This is because the PES is sensitive only to the way the ground state CSFs are distributed in the core hole state [Eq. (3)]. The AES, instead, is sensitive to the amount of each CSF in the intermediate ionic state, to the orbitals involved, and to the signs of the Auger amplitudes [Eq. (4)].

We are grateful to the staff of the MAX Laboratory for help during the measurements. Financial support from the National Gradute School in Materials Physics, the Vilho, Yrjö and Kalle Väisälä Foundation, the Oulu University Scholarship Foundation, the European Community Access to Research Infrastructure Action of the Improving Human Potential Program, and the Research Council for the Natural Sciences of the Finnish Academy is acknowledged.

[1] J. M. Bizau, D. Cubaynes, P. Gérard, and F. J. Wuilleumier, Phys. Rev. A **40**, 3002 (1989).
[2] M. Richter, M. Meyer, M. Pahler, T. Prescher, E. Raven, B. Sonntag, and H. E. Wetzel, Phys. Rev. A **39**, 5666 (1989).
[3] A. Mäntykenttä, H. Aksela, S. Aksela, J. Tulkki, and T. Åberg, Phys. Rev. A **47**, 4865 (1993).
[4] T. Matila and H. Aksela, J. Phys. B **33**, 653 (2000).
[5] G. Snell, M. Martins, E. Kukk, W. T. Cheng, and N. Berrah, Phys. Rev. A **63**, 062715 (2001).
[6] T. X. Carrolll, J. D. Bozek, E. Kukk, V. Myrseth, L. J. Saethre, T. D. Thomas, and K. Wiesner, J. Electron Spectrosc. Relat. Phenom. **125**, 127 (2002).
[7] F. A. Parpia, C. Froese Fisher, and I. P. Grant, Comput. Phys. Commun. **94**, 249 (1996).
[8] S. Fritzsche, J. Electron Spectrosc. Relat. Phenom. **114**, 1155 (2001).